Available online at www.sciencedirect.com
ScienceDirect
Procedia Computer Science 00 (2010) 1–10
Procedia Computer Science

International Conference on Computational Science, ICCS 2011

Meso-GSHMC: A stochastic algorithm for meso-scale constant temperature simulations

Elena Akhmatskaya[a,1], Sebastian Reich[b]

[a] *Fujitsu Laboratories of Europe Ltd, Hayes Park Central, Hayes End Road, Hayes, Middlesex, UB4 8FE, UK, and Basque Center for Applied Mathematics, Bizkaia Technology Park, Building 500, E48160, Derio, Spain*
[b] *Universität Potsdam, Institut für Mathematik, Am Neuen Palais 10, D-14469, Potsdam, Germany*

Abstract

We consider the problem of time-stepping/sampling for molecular and meso-scale particle dynamics. The aim of the work is to derive numerical time-stepping methods that generate samples exactly from the desired target temperature distribution. The numerical methods proposed in this paper rely on the well-known splitting of stochastic thermostat equations into a conservative and a fluctuation-dissipation. We propose a methodology to derive numerical approximation to the fluctuation-dissipation part that exactly samples from the underlying Boltzmann distribution. Our methodology applies to Langevin dynamics as well as Dissipative Particle Dynamics and, more generally, to arbitrary position dependent fluctuation-dissipation terms. A Metropolis criterion is introduced to correct for numerical inconsistency in the conservative dynamics part of the model. Shadow energies are used to increase the acceptance rate under the Metropolis criterion. We call the newly proposed method meso-GSHMC.

Keywords: Dissipative Particle Dynamics, Monte Carlo methods, constant temperature simulation

1. Introduction

Classical molecular dynamics (MD) simulations of all-atoms or coarse grained systems are among the most popular techniques for simulation of soft matter. Classical MD simulations are naturally performed under the conditions of constant energy E, constant volume V, and constant number of particles N. One refers to such simulations as microcanonical or NVE ensemble simulations [1, 2]. In addition to energy, volume and number of particles, microcanonical ensemble simulations also conserve linear and angular momentum, with the later not being a constant under periodic boundary conditions. Unfortunately, the microcanonical (NVE) ensemble does not correspond to the conditions under which most experiments are carried out. If one is interested in the behavior of the system at a specific temperature T, a constant NVT ensemble simulation using a thermostat is required. See, for example, [1, 2] for a description of popular thermostats. In this paper, we focus on stochastic thermostats (e.g., the Andersen thermostat, Langevin and Dissipative Particle Dynamics (DPD)) and their numerical implementation since these methods appear to be robust and accurate in a wide range of applications [1, 2].

[1] Corresponding author

Note that local thermostats, such as Langevin dynamics and DPD, can be viewed as simplified reduced systems in the sense of Mori-Zwanzig reduction (see, for example, [1]). This aspect is particularly important for coarse grained models for which the fluctuation-dissipation contributions should not only keep the system at a desired target temperature but should also mimic the impact of non-resolved finer details of an all-atom model on the coarse grained length and time scales. Under those circumstances, the appropriate numerical treatment of fluctuation-dissipation terms also gains in importance.

The numerical methods proposed in this paper rely on the well-known splitting of stochastic thermostat equations into a conservative and a fluctuation-dissipation part [1]. We propose a methodology to derive numerical approximation to the fluctuation-dissipation part that exactly samples from the underlying Boltzmann distribution. Our methodology applies to Langevin dynamics as well as DPD and, more generally, to arbitrary position dependent fluctuation-dissipation terms. A composition method approach is used to derive a time-stepping method for the complete thermostat, where the conservative dynamics part is discretized by the standard Störmer-Verlet method [1, 3]. A Metropolis criterion is introduced to correct for inconsistency in the Störmer-Verlet time-stepping method with the underlying NVT ensemble and puts the resulting propagator into the context of Markov chain Monte Carlo (MCMC) methods [4]. Our approach relies essentially on an appropriate adaptation of the generalized hybrid Monte Carlo method of [5, 6]. Acceptance rates under the Metropolis criterion can be increased using shadow energies as demonstrated in the work of [7, 8]. The proposed methods are applicable to meso-scale and coarse grained molecular dynamics simulations which require a highly accurate sampling from the given target NVT ensemble.

Following [8], the techniques proposed in this paper can be combined with constant temperature T, pressure P, and number of particles N (NPT) ensemble simulation techniques such as proposed by [9, 10].

An outline of the paper is as follows. The stochastic equations of second-order Langevin and dissipative particle dynamics (DPD) are summarized in Section 2. We also provide a summary of state of the art numerical methods for stochastic thermostats and discuss shadow energies [11, 3] for conservative time-stepping methods such as Störmer-Verlet. Numerical methods which exactly sample from the velocity Boltzmann distribution for force-free motion are proposed in Section 3, where we also discuss their composition with the Störmer-Verlet method for conservative dynamics. Since the composed approximation does not exactly sample from the NVT ensemble, a Metropolis corrected implementation, based on the generalized shadow hybrid Monte Carlo (GSHMC) method [8], is proposed in Section 4. The new method is called meso-GSHMC. Numerical results for a standard DPD test case as well as from a membrane protein simulation are provided in Section 5. Concluding remarks can be found in Section 6.

We finally mention that Monte Carlo methods such as meso-GSHMC can be put into the context of massively parallel computing. A first approach is to use massively parallel implementations of the necessary force field calculations. A second application arises when Monte Carlo chains are conducted in parallel and independently. More parallelization strategies arise as refinements of this trivial (but often very useful) exploitation of parallelism. Such refinements include parallel tempering/replica exchange and orientational bias Monte Carlo [4].

2. Summary of local stochastic thermostat formulations

We consider an N-atom molecular system with atomistic positions $\mathbf{r}_i = (x_i, y_i, z_i)^T \in \mathbb{R}^3$, velocities $\mathbf{v}_i = (u_i, v_i, w_i)^T \in \mathbb{R}^3$, masses m_i, momenta $\mathbf{p}_i = m_i\mathbf{v}_i \in \mathbb{R}^3$, potential energy function V, and total energy function

$$E = \frac{1}{2}\sum_{i=1}^{N}\frac{\|\mathbf{p}_i\|^2}{m_i} + V(\mathbf{r}_1, \mathbf{r}_2, \ldots, \mathbf{r}_N). \tag{1}$$

For easy of reference, we introduce the notations $\mathbf{r} = (\mathbf{r}_1^T, \ldots, \mathbf{r}_N^T)^T \in \mathbb{R}^{3N}$, $\mathbf{v} = (\mathbf{v}_1^T, \ldots, \mathbf{v}_N^T)^T \in \mathbb{R}^{3N}$, $\mathbf{p} = (\mathbf{p}_1^T, \ldots, \mathbf{p}_N^T)^T \in \mathbb{R}^{3N}$, and a diagonal mass matrix $M \in \mathbb{R}^{3N\times 3N}$ such that the energy conserving microcanonical equations of motion can be written in compact form as

$$\frac{\mathrm{d}\mathbf{r}}{\mathrm{d}t} = M^{-1}\mathbf{p}, \qquad \frac{\mathrm{d}\mathbf{p}}{\mathrm{d}t} = -\nabla_{\mathbf{r}}V(\mathbf{r}). \tag{2}$$

We now introduce a unifying framework for locally coupled stochastic thermostats, which allow one to convert (2) to formulations suitable for constant temperature (NVT ensemble) simulations.

2.1. Langevin and dissipative particle dynamics (DPD)

DPD has become a very popular method for meso-scale simulations of materials. In this section, we provide a short summary of the method and discuss a slightly more general framework that also includes traditional Langevin dynamics. Following the notation of [12], the standard DPD method of [13] can be formulated as a stochastic differential equation (SDE):

$$\mathrm{d}\mathbf{r}_i = \frac{\mathbf{p}_i}{m_i}\,\mathrm{d}t, \qquad \mathrm{d}\mathbf{p}_i = \left[\mathbf{F}_i - \gamma \sum_{j\neq i} \omega(r_{ij})(\mathbf{e}_{ij}\cdot\mathbf{v}_{ij})\mathbf{e}_{ij}\right]\mathrm{d}t + \sigma \sum_{j\neq i} \omega^{1/2}(r_{ij})\mathbf{e}_{ij}\,\mathrm{d}W_{ij}, \tag{3}$$

where $\mathbf{r}_{ij} = \mathbf{r}_i - \mathbf{r}_j$, $r_{ij} = |\mathbf{r}_i - \mathbf{r}_j|$, $\mathbf{e}_{ij} = \mathbf{r}_{ij}/r_{ij}$, $\mathbf{v}_{ij} = \mathbf{v}_i - \mathbf{v}_j$, and $\mathbf{F}_i = -\nabla_{\mathbf{r}_i} V(\mathbf{r})$ is the conservative force acting on particle i. The dimensionless weight function $\omega(r)$ can be chosen in a rather arbitrary manner. However, to reproduce a constant temperature ensemble, the friction coefficient γ and the noise amplitude σ have to satisfy the fluctuation dissipation relation $\sigma = \sqrt{2k_BT\gamma}$. Here k_B denotes the Boltzmann constant. Finally, $W_{ij}(t) = W_{ji}(t)$ are independent Wiener processes [14]. Recall that the finite-time increments $\Delta W_{ij}(\tau) = W_{ij}(t+\tau) - W_{ij}(t)$ of a Wiener process are Gaussian distributed with mean zero and variance $\sqrt{\tau}$, i.e., $\Delta W_{ij}(\tau) \sim \mathrm{N}(0,\tau)$, where $\mathrm{N}(a,b)$ denotes the Gaussian distribution with mean a and variance b.

Following [15], let us write the equations (3) in a more compact and general manner:

$$\mathrm{d}\mathbf{r} = M^{-1}\mathbf{p}\,\mathrm{d}t, \qquad \mathrm{d}\mathbf{p} = -\nabla_{\mathbf{r}} V(\mathbf{r})\,\mathrm{d}t - \sum_{k=1}^{K} \nabla_{\mathbf{r}} h_k(\mathbf{r})\left[\gamma \dot{h}_k(\mathbf{r})\,\mathrm{d}t - \sigma\,\mathrm{d}W_k\right], \tag{4}$$

where

$$\dot{h}_k(\mathbf{r}) = \nabla_{\mathbf{r}} h_k(\mathbf{r})\cdot\mathbf{v} = \nabla_{\mathbf{r}} h_k(\mathbf{r})\cdot M^{-1}\mathbf{p}, \tag{5}$$

and the functions $h_k(\mathbf{r})$, $k = 1,\ldots,K$, can be chosen quite arbitrarily. The choice $h_k(\mathbf{r}) = \phi(r_{ij})$, $\phi'(r) = \omega^{1/2}(r)$, $k = 1,\ldots,K$, with $K = (N-1)N/2$ in (4) leads back to the standard DPD model. However, one can also set $K = 3N$ and derive the standard Langevin model.

An intriguing aspect of the DPD equations (3) is that they satisfy Newton's third law which implies conservation of total linear and angular momentum. The same is not true for Langevin dynamics. Conservation of total linear and angular momentum has made DPD a popular method for meso-scale simulations (see, e.g., [16]) as well as a stochastic thermostat for NVT simulations [17].

2.2. State of the art numerical treatment

Appropriate time-stepping methods for the conservative part (2) form the basis of any time-stepping methods for stochastic thermostats. It seems that there is widespread agreement that the conservative part should be solved numerically by the Störmer-Verlet method, which is written here in the velocity/momentum formulation:

$$\mathbf{p}^{n+1/2} = \mathbf{p}^n - \frac{\Delta t}{2}\nabla_{\mathbf{r}} V(\mathbf{r}^n), \quad \mathbf{r}^{n+1} = \mathbf{r}^n + \Delta t \mathbf{M}^{-1}\mathbf{p}^{n+1/2}, \quad \mathbf{p}^{n+1} = \mathbf{p}^{n+1/2} - \frac{\Delta t}{2}\nabla_{\mathbf{r}} V(\mathbf{r}^{n+1}), \tag{6}$$

where Δt is the step size. The method was first used in the context of MD by Verlet [18] and has been very popular with the MD community since [1].

Why is the Störmer-Verlet method so successful for constant energy MD simulations? Several reasons can be given. The method is easy to implement, it exactly conserves total linear and angular momentum, it is time-reversible, it conserves volume of phase space $\Omega = \mathbb{R}^{3N}$, and the total energy (1) is very well conserved over long simulation times even for large and complex systems. Near conservation of energy is due to the existence of shadow energies which are preserved to much higher order than the method itself. See [11, 3] for a detailed theoretical exploration of this phenomena. An explicit algorithm for computing shadow (also called modified) energies along numerically computed trajectories can be found in [19]. In an numerical experiment we demonstrate conservation of energy under the Störmer-Verlet method applied to the microcanonical equations (2). For simplicity, we consider a one-dimensional period chain of $N = 10$ particles with interacting through a pair-wise Lennard-Jones potential. Relative changes in the numerical values of the energy (1) as well as fourth and eighth-order shadow energies from [19], respectively, can be found in Figure 1. Shadow energies can be used, for example, to assess the quality of NVE ensemble simulations

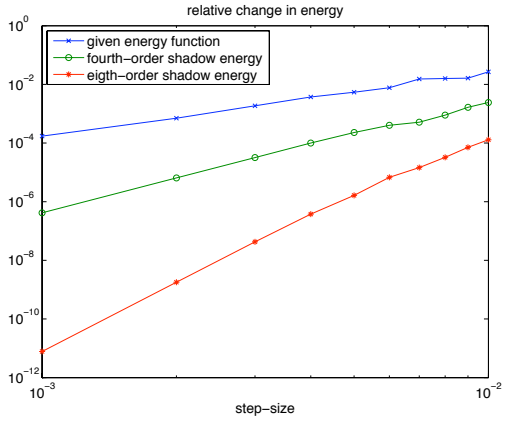

Figure 1: Displayed are relative changes in the total energy and fourth and eighth-order shadow energies as a function of the step-size Δt. Simulations are performed with the Störmer-Verlet method for a one-dimensional chain of Lennard-Jones particles. The slope of the graphs correctly reflects the order of the method and its shadow energies for sufficiently small step-sizes.

[20] and to increase the acceptance rate in Markov chain Monte Carlo methods based on molecular dynamics proposal steps [21, 7, 8].

While Störmer-Verlet is the gold standard for NVE simulations, the optimal numerical treatment of the DPD equations (3), on the other hand, is still a subject of debate. See, for example, [22, 23, 24, 25, 26, 27, 28, 29, 17, 30]. For a comparison of several numerical algorithms for DPD see [26, 27]. In particular, it is found that the numerically observed temperature T^* depends on the step-size Δt and differs from the target temperature T. Methods are now available that lead to $T^* = T$ in the absence of conservative forces [23, 28, 17, 30]. However, none of the existing methods leads to $T^* = T$ under the full DPD dynamics.

3. A splitting approach for stochastic thermostats

In this section, we develop a general framework for numerical implementation of stochastic thermostats. The approach is based on a splitting of the stochastic differential equation into an energy conserving part and fluctuation-dissipation part. This splitting is used since each part separately conserves the canonical distribution

$$\rho_{\text{can}}(\mathbf{q},\mathbf{p}) \propto \exp\left(-\frac{1}{k_B T} E(\mathbf{q},\mathbf{p})\right) \tag{7}$$

under its analytically generated Markov processes.

3.1. Treatment of fluctuation-dissipation part

While splitting methods have been discussed in the context of stochastic differential equations before (see, for example, [31, 32, 33, 25, 34, 30, 35]), we propose to use simplified numerical methods for the fluctuation-dissipation contributions which, however, exactly conserve the momentum Boltzmann distribution [1]. We next describe these methods in the context of DPD and consider the DPD-type force free momentum dynamics

$$\mathrm{d}\mathbf{p} = -\sum_{k=1}^{K} \nabla_{\mathbf{r}} h_k(\mathbf{r}) \left[\gamma \dot{h}_k(\mathbf{r})\,\mathrm{d}t - \sigma\,\mathrm{d}W_k\right] \tag{8}$$

for fixed position vector $\mathbf{r}$. Note that (8) constitutes a linear SDE. Again the goal is to devise numerical approximations $\{\mathbf{p}^n\}$ at $t_n = n\,\Delta t$, $n = 0, \ldots N_{\text{steps}}$, N_{steps} the number of time-steps, that possess the Boltzmann velocity distribution as the stationary distribution. To achieve this goal, we propose to consider

$$\frac{\mathrm{d}\mathbf{p}}{\mathrm{d}s} = \sum_{k=1}^{K} \nabla_{\mathbf{r}} h_k(\mathbf{r})\, R_k, \qquad \frac{\mathrm{d}R_k}{\mathrm{d}s} = -\nabla_{\mathbf{r}} h_k(\mathbf{r}) \cdot M^{-1}\mathbf{p}, \qquad k = 1, \ldots, K, \tag{9}$$

as a generating differential equation for the fluctuation-dissipation part of the general DPD formulation (4). The initial $R_k(0)$ are Gaussian random numbers with mean zero and variance k_BT, i.e. $R_k(0) \sim \mathrm{N}(0, k_BT)$ for $i = 1, \ldots, K$. We introduce the notation $\mathbf{R} = (R_1, \ldots, R_K)^T$.

To obtain a numerical momentum update step, we seek the solution at $s = \sqrt{2\gamma\Delta t}$ for given initial conditions $\mathbf{p}(0) = \mathbf{p}^n$, $R_k(0) = R_k^n = \mathrm{N}(0, k_BT)$, $k = 1, \ldots, K$. Let us denote the linear solution operator, generated by the solutions of (9), by $\mathcal{R}(s) \in \mathbb{R}^{(3N+K)\times(3N+K)}$. The solution operator $\mathcal{R}(s)$ has the following properties [3]: (a) The solutions of (9) are volume conserving, i.e., $\det \mathcal{R}(s) = 1$. (b) Given a fixed position vector $\mathbf{r}$, the solutions of (9) are time reversible, i.e., $\mathcal{F}\mathcal{R}(s)\mathcal{F} = \mathcal{R}(-s)$. Here $\mathcal{F}$ denotes the linear involution operator that changes the sign of all R_k's, $k = 1, \ldots, K$. (c) The solutions of (9) conserve the extended Hamiltonian/energy

$$E_c = \frac{1}{2}\left(\mathbf{p}^T M^{-1}\mathbf{p} + \mathbf{R}^T\mathbf{R}\right). \tag{10}$$

(d) Properties (a) and (c) immediately imply that the solutions of (9) conserve the extended canonical distribution

$$\pi_c(\mathbf{p}, \mathbf{R}) \propto e^{-\beta E_c}. \tag{11}$$

We now consider the numerical implementation of (9). To do so we follow the hybrid Monte Carlo (HMC) methodology [36, 37] and consider time-reversible and volume conserving propagators for the dynamics in $\mathbf{p}$ and $\mathbf{R}$ with fixed position vector $\mathbf{r}$. Two such methods will be considered: (i) an explicit one, which does not conserve (10), and (ii) an implicit one, which does conserve (10).

Störmer-Verlet method. A first choice is provided by the application of the Störmer-Verlet method to (9) over J internal steps with internal step-size $\Delta s = \sqrt{2\gamma\Delta t}/J$ and we obtain

$$\mathbf{p}^{j+1/2} = \mathbf{p}^j + \frac{\Delta s}{2}\sum_{k=1}^{K}\nabla_{\mathbf{r}} h_k(\mathbf{r})R_k^j, \tag{12}$$

$$R_k^{j+1} = R_k^j - \Delta s\nabla_{\mathbf{r}} h_k(\mathbf{r})\cdot M^{-1}\mathbf{p}^{j+1/2}, \qquad k = 1, \ldots, K, \tag{13}$$

$$\mathbf{p}^{j+1} = \mathbf{p}^{j+1/2} + \frac{\Delta s}{2}\sum_{k=1}^{K}\nabla_{\mathbf{r}} h_k(\mathbf{r})R_k^{j+1}. \tag{14}$$

The final result, denoted by $\mathbf{p}' = \mathbf{p}^J$ and $R_k' = R_k^J$, $k = 1, \ldots, K$, is accepted with probability

$$r = \min\left(1, \frac{\pi(\mathbf{p}', \mathbf{R}')}{\pi(\mathbf{p}^n, \mathbf{R}^n)}\right). \tag{15}$$

In case of rejection, we continue with the initial $\mathbf{p}^n$; i.e., in case of rejection we have $\mathbf{p}^{n+1} = \mathbf{p}^n$. Otherwise we set $\mathbf{p}^{n+1} = \mathbf{p}'$. In line with the standard HMC method, the vector $\mathbf{R}'$ is entirely discarded after each completed momentum update step.

Note that the acceptance probability $r \to 1$ as $\Delta s \to 0$. This follows from the convergence of the numerical propagator to the exact $\mathcal{R}(s)$ as $\Delta s \to 0$. Hence, as a rule of thumb, we suggest to pick J large enough such that the rejection rate in (15) becomes negligible (e.g., less than 1%) for given $s = \sqrt{2\gamma\Delta t}$.

Implicit midpoint rule. An alternative propagator is obtained by applying the implicit midpoint rule (see, e.g., [3]) to (9) over a single step with step-size $\Delta s = \sqrt{2\gamma\Delta t}$ and we obtain

$$\mathbf{p}' = \mathbf{p} + \frac{\Delta s}{2}\sum_{k=1}^{K}\nabla_{\mathbf{r}} h_k(\mathbf{r})(R_k' + R_k), \tag{16}$$

$$R_k' = R_k - \frac{\Delta s}{2}\nabla_{\mathbf{r}} h_k(\mathbf{r})\cdot M^{-1}(\mathbf{p}' + \mathbf{p}), \qquad k = 1, \ldots, K. \tag{17}$$

The resulting linear equations in $(\mathbf{p}', \mathbf{R}')$ can be solved by a simple fixed point iteration or some other iterative solver. Since only matrix vector multiplications are involved and the matrices involved are typically very sparse, such iterative methods can be implemented efficiently especially on parallel computers.

An appealing aspect of the implementation (16)-(17) is that it conserves the extended energy (10) exactly and, hence, also the corresponding canonical distribution function (11). Since the method also conserves volume and is time-reversible, the proposed momenta $\mathbf{p}'$ are always accepted, while the vector $\mathbf{R}'$ is entirely discarded after each momentum update step.

Because of the necessary fixed point iteration, the implicit midpoint method (16)-(17) is more expensive than the Störmer-Verlet method ((12)-(14). However, we nevertheless recommend the implicit midpoint method because of the ideal acceptance probability $r = 1$.

3.2. Treatment of conservative part

Since the Störmer-Verlet method does not conserve energy exactly, it also does not conserve the canonical distribution (7). Hence, in the context of our splitting method, we need to correct the Störmver-Verlet discretization of the conservative part of the dynamics such that the canonical distribution (7) is preserved. This is essentially the approach taken by the generalized hybrid Monte Carlo (GHMC) method of [5, 6]. To make GHMC applicable to DPD type stochastic thermostats, we combine the newly proposed momentum updates (Section 3.1) with a Metropolis acceptance/rejection criterions for the conservative dynamics update. Furthermore, to increase the acceptance rate in the conservative dynamics part of GHMC we utilize the idea of shadow energies as employed by the generalized shadow hybrid Monte Carlo (GSHMC) method [8]. The details are described in the following section. We call the resulting method meso-GSHMC.

4. The meso-GSHMC method

In this section, we demonstrate how to extend the GHMC methodology to DPD-type momentum updates such that the resulting Markov chain Monte Carlo (MCMC) method samples exactly from the canonical distribution (7).

The key idea of the generalized shadow hybrid Monte Carlo (GSHMC) method of [8] is to assess the Monte Carlo steps of GHMC with regard to a shadow Hamiltonian $\mathcal{E}_{\Delta t}$, which increases the acceptance rate in the conservative dynamics part of GHMC. A shadow energy can either be found using the methods of [7, 8] or [19].

We now outline the meso-GSHMC method. While the conservative dynamcis part of meso-GSHMC is identical to the approach described in [8] for GSHMC, we need to reconsider the momentum refreshment step.

4.1. Momentum refreshment step

When using shadow energies, we need to modify the partial momentum update step, as defined by (16)-(17) (in case of the implicit midpoint implementation). More specifically, given a shadow energy $\mathcal{E}_{\Delta t}$, the key idea is to replace the extended canonical density (11) by

$$\widehat{\pi}(\mathbf{r}, \mathbf{p}, \mathbf{R}) \propto \exp\left(-\beta \mathcal{E}_{\Delta t}(\mathbf{r}, \mathbf{p}) - \beta/2 \sum_{k=1}^{K} (R_k)^2\right), \tag{18}$$

and the acceptance probability (15) by

$$r = \min\left(1, \frac{\widehat{\pi}(\mathbf{r}, \mathbf{p}', \mathbf{R}')}{\widehat{\pi}(\mathbf{r}, \mathbf{p}, \mathbf{R})}\right). \tag{19}$$

Recall that if $\mathcal{E}_{\Delta t} = E$, then $r = 1$ for the implicit midpoint implementation (16)-(17).

Since the meso-GSHMC method samples with respect to a modified canonical ensemble, it is necessary to reweight the computed samples $\{\Omega_j\}$ of an observable $\Omega = \Omega(\mathbf{r}, \mathbf{p})$. See [7, 8] and the algorithmic summary below for details.

4.2. Meso-GSHMC: Algorithmic summary

The meso-GSHMC method is defined through an energy/Hamiltonian (1), a shadow energy $\mathcal{E}_{\Delta t}$, inverse temperature $\beta = 1/k_B T$, a set of position-dependent functions $\{h_k(\mathbf{r})\}_{k=1}^{K}$, friction constant γ, time-step Δt, and number of time-steps L. The method generates a sequence of states Γ^j, $j = 1, \ldots, J$. We now summarize a single step of the meso-GSHMC method.

(i) *Conservative dynamics step.* Given the last accepted state Γ^j with a pair of position and momentum vectors $(\mathbf{r}, \mathbf{p})$, we numerically integrate the Hamiltonian equations of motion (2) over L time-steps with the Störmer-Verlet method (6) step-size Δt, and initial conditions $\mathbf{r}^0 = \mathbf{r}$, $\mathbf{p}^0 = \mathbf{p}$. This results in the approximation $(\mathbf{r}^L, \mathbf{p}^L)$. The accepted pair of position and momentum vectors $(\bar{\mathbf{r}}, \bar{\mathbf{p}})$ is obtained via the Metropolis accept/reject test

$$(\bar{\mathbf{r}}, \bar{\mathbf{p}}) = \begin{cases} (\mathbf{r}^L, \mathbf{p}^L) & \text{with probability } \min(1, \exp(-\beta\, \delta\mathcal{E}_{\Delta t})) \\ (\mathbf{r}^0, -\mathbf{p}^0) & \text{otherwise} \end{cases}, \tag{20}$$

where

$$\delta\mathcal{E}_{\Delta t} := \mathcal{E}_{\Delta t}(\mathbf{r}^L, \mathbf{p}^L) - \mathcal{E}_{\Delta t}(\mathbf{r}^0, \mathbf{p}^0). \tag{21}$$

(ii) *Momentum refreshment step.* A sequence of i.i.d. random numbers $R_k \sim \mathrm{N}(0, \beta^{-1})$, $k = 1, \ldots, K$, is generated. Using the implicit midpoint rule implementation of the momentum refreshment step, the system (16)-(17) is solved for $(\mathbf{p}', \mathbf{R}')$ by fixed point iteration and initial momentum $\mathbf{p} = \bar{\mathbf{p}}$ and fixed position $\mathbf{r} = \bar{\mathbf{r}}$. The accepted momentum vector $\mathbf{p}''$ is obtained via the Metropolis criterion

$$\mathbf{p}'' = \begin{cases} \mathbf{p}' & \text{with probability } \min(1, \exp(-\beta\, \delta\mathcal{E}_{\Delta t,\mathrm{ext}})) \\ \bar{\mathbf{p}} & \text{otherwise} \end{cases}, \tag{22}$$

where

$$\delta\mathcal{E}_{\Delta t,\mathrm{ext}} := \left[\mathcal{E}_{\Delta t}(\bar{\mathbf{r}}, \mathbf{p}') + \frac{1}{2}\sum_{k=1}^{K}(R_k')^2\right] - \left[\mathcal{E}_{\Delta t}(\bar{\mathbf{r}}, \bar{\mathbf{p}}) + \frac{1}{2}\sum_{k=1}^{K}(R_k)^2\right]. \tag{23}$$

(iii) The newly accepted pair of position and momentum vectors is provided by $\bar{\mathbf{r}}$ (from the conservative dynamics part) and $\mathbf{p}''$ (from the momentum refreshment step), respectively, and give rise to Γ^{j+1}.

Under the assumption of ergodicity of the induced Markov chain, the ensemble average of an observable $\Omega(\Gamma) = \Omega(\mathbf{r}, \mathbf{p})$ with respect to the canonical ensemble (7) is approximated as

$$\langle\Omega\rangle = \frac{\sum_{j=1}^{J} w_j \Omega(\Gamma^j)}{\sum_{j=1}^{J} w_j} \tag{24}$$

where $w_j = \exp\left(\beta\left[\mathcal{E}_{\Delta t}(\Gamma^j) - E(\Gamma^j)\right]\right)$.

4.3. Remarks

It should be noted that the Metropolis criterion (20) leads to a trajectory reversal upon rejection of the conservative dynamics proposal step; i.e., the method continues with the previous position vector $\mathbf{r}^0$ and negated momentum vector $\mathbf{p}^0$ upon rejection of the proposal step. While this trajectory reversal is required for detailed balance with respect to the canonical distribution (7) it also implies that rejections interfere strongly with the dynamics. It has been proposed by [38] to replace (20) by

$$(\bar{\mathbf{r}}, \bar{\mathbf{p}}) = \begin{cases} (\mathbf{r}^L, \mathbf{p}^L) & \text{with probability } \min(1, \exp(-\beta\, \delta E)) \\ (\mathbf{r}^0, \mathbf{p}^0) & \text{otherwise} \end{cases}. \tag{25}$$

Unfortunately, detailed balance does no longer holds under (25) [39]. However, it has been demonstrated for simple test problems that (25) increases the sampling accuracy and interferes less with the dynamics of the stochastic thermostats than (20) [38, 39]. See also [40] for related results on Metropolis corrected stochastic Nosé-Hoover dynamics [41]. In this paper, we implement meso-GHMC with the Metropolis criterion (20) to demonstrate exact sampling from the canonical distribution (7).

We emphasize that meso-GSHMC can also be implemented with the shadow energy being the original energy (1). In this case, it is more appropriate to call the resulting Monte Carlo method meso-GHMC.

5. Numerical results

5.1. DPD test system

Numerical results from the meso-GHMC/GSHMC methods are compared to the MD-VV implementation [26] of DPD. Numerical experiments are conducted for Model C of [26]. For the chosen units, we have $k_BT = 1$ in dimensionless variables. Model C is a simple interacting Lennard-Jones fluid with truncated pairwise interaction potential

$$U(\mathbf{r}_{ij}) = \begin{cases} 4\left[\left(\frac{l}{r_{ij}}\right)^{12} - \left(\frac{l}{r_{ij}}\right)^{6}\right], & r_{ij} \le r_c, \\ 0, & r_{ij} > r_c, \end{cases} \tag{26}$$

with $r_c = 1$ and $l = 2^{-1/6}$. The simulation box is of size 16×16×16 with a total of $N = 2867$ particles. This corresponds to a density of $\rho = 0.7$. The conservative dynamics part is implemented with $\tau = 0.05$ and varying values for Δt and, hence, $L = \tau/\Delta t$, while the momentum refreshment step is implemented with $\Delta s = (2\gamma\tau)^{1/2} \approx 4.4721$ in (16)-(17) with $\gamma = 200$ ($\sigma = 20$, respectively).

The meso-GSHMC method is implemented with a fourth-order accurate shadow energy as $\mathcal{E}_{\Delta t}$. The numerical experiments are conducted with the fourth-order shadow energy of [8]. Note that the truncated interaction potential (26) leads to a continuous only force field. Higher regularity of the force fields is required to achieve a fourth-order accuracy in the shadow energy. The fourth-order behavior is indeed not observed in our numerical experiments. See [29] for the use of smoother truncation schemes in the context of DPD. The reference experiments with the standard DPD method of [26] use the same parameter settings.

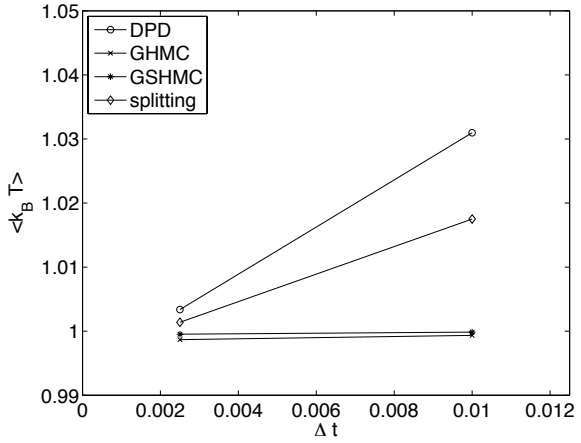

Figure 2: Numerically observed temperature $\langle k_BT\rangle$ vs the step-size Δt in Model C. Results are obtained from a standard DPD integration scheme and the newly proposed meso-GHMC/GSHMC methods. The correct result is $\langle k_BT\rangle = 1$. We also display the temperature obtained from the proposed splitting approach, where the non-conservation of energy under the Störmer-Verlet method is not corrected by a Metropolis accept/reject step.

We confirm in Fig. 2 that the newly proposed meso-GSHMC/GHMC methods reproduce the target value $k_BT = 1$ under the full dynamics. We also find that the splitting approach of Section 3 leads to a drift in temperature due to the non-conservation of the canonical distribution (7) under the Störmer-Verlet discretization of the conservative dynamics part of DPD.

5.2. Membrane protein

Meso-scale simulations techniques are increasingly applied to problems from biophysical chemistry such as the interaction of macromolecules with the interface between an aqueous solution and biological membranes; i.e., phospholipid bilayer. These simulations are based on coarse-grained (CG) approaches which replace the all atom classical mechanics force-fields of traditional molecular dynamics. As an example we mention the studies of [42, 43, 44] on CG simulations of simple peptides and integral membranes interacting with a lipid bilayer. In addition to finding

more accurate CG force fields, there also remains the need to improve accuracy and efficiency of sampling to guarantee convergence of CG simulations. Since CG simulations are typically performed in a NVT ensemble setting, stochastic thermostats such as those considered in this paper can be applied. A comparison between standard constant temperature CG-MD simulations using a Berendsen thermostat with the GSHMC method, as described in this paper, has been conducted in [45]. The test application is a gating-modifier peptide toxin in a membrane with environment. See [45] for a detailed description of the model system, simulation set-up, and numerical results. In Figure 3, the evolution of the toxin is shown from an initial position within the membrane to its preferred position at the surface of the bilayer. The GSHMC method leads to a much more rapid repositioning of the toxin compared to a CG-MD simulation with Berendsen thermostat.

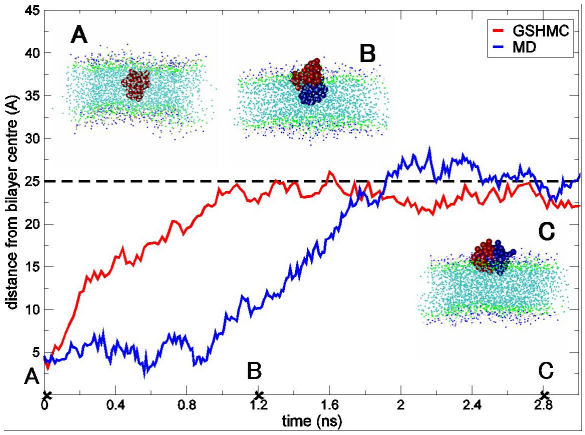

Figure 3: Displayed is the evolution of peptide toxin from an initial position within the membrane to its preferred position at the surface of the membrane. More specifically, the distance of the toxin to an energy minimized reference position at the surface of the membrane is shown for a CG-MD and a GSHMC simulation. While both simulation methods correctly identify the preferred location of the toxin, the toxin equilibrates much faster under the GSHMC simulation.

6. Concluding remarks

In this paper, we have investigated local stochastic thermostats such as Langevin and dissipative particle dynamics. We have proposed simple modifications to existing methods which sample exactly from the Boltzmann distribution for position-dependent fluctuation-dissipation terms and force free motion. Alternative methods with the same property have been proposed in the past but rely on a splitting into pairwise interactions [23, 25, 28, 17] and can therefore not easily be applied to very large systems. As another novel contribution, we have also shown how to put stochastic thermostats with position-dependent fluctuation-dissipation terms, for example DPD, within the framework of Markov chain Monte Carlo methods which implies rigorous sampling from the canonical distribution (7) regardless of the chosen step-size Δt. We have verified this property numerically for Model C from [26]. We have also demonstrated for a membrane protein system that Metropolis corrected time-stepping methods are efficient for applications which require a careful and rapid equilibration with respect to a given target temperature.

The proposed methods can be viewed as Metropolis corrected time-stepping methods similar to the HMC scheme for first-order Brownian dynamics. However, it should be noted that the Metropolis test induces non-trivial changes to the dynamics in case of rejection of the proposal step. A possible compromise between sampling accuracy and reduced interference with dynamics is to remove the momentum reversal upon rejection in (20), respectively, from the meso-GHMC/GSHMC methods and to use a Metropolis test of type (25). See [38, 39] for some initial results, which indicate that GHMC/GSHMC without momentum flip improves the accuracy of standard time-stepping methods while interfering little with dynamic properties such as autocorrelation functions provided the acceptance rate is kept sufficiently high. This aspect requires further investigations.

[1] M. Allen, D. Tildesley, Computer Simulation of Liquids, Clarendon Press, Oxford, 1987.
[2] D. Frenkel, B. Smit, Understanding Molecular Simulation, 2nd Edition, Academic Press, New York, 2001.

[3] B. Leimkuhler, S. Reich, Simulating Hamiltonian Dynamics, Cambridge University Press, Cambridge, 2005.
[4] J. Liu, Monte Carlo Strategies in Scientific Computing, Springer-Verlag, New York, 2001.
[5] A. Horowitz, A generalized guided Monte-Carlo algorithm, Phys. Lett. B 268 (1991) 247–252.
[6] A. Kennedy, B. Pendleton, Cost of the generalized hybrid Monte Carlo algorithm for free field theory, Nucl. Phys. B 607 (2001) 456–510.
[7] E. Akhmatskaya, S. Reich, The targeted shadowing hybrid Monte Carlo (TSHMC) method, in: B. L. et al (Ed.), New Algorithms for Macromolecular Simulations, Vol. 49 of Lecture Notes in Computational Science and Engineering, Springer-Verlag, Berlin, 2006, pp. 145–158.
[8] E. Akhmatskaya, S. Reich, GSHMC: An efficient method for molecular simulations, J. Comput. Phys. 227 (2008) 4934–4954.
[9] H. Andersen, Molecular dynamics simulations at constant pressure and/or temperature, J. Chem. Phys. 72 (1980) 2384–2393.
[10] S. Feller, Y. Zhang, R. Pastor, B. Brooks, Constant pressure molecular dynamics: The Langevin piston method, J. Chem. Phys. 103 (1995) 4613–4621.
[11] E. Hairer, C. Lubich, G. Wanner, Geometric Numerical Integration, Springer-Verlag, Berlin Heidelberg, 2002.
[12] P. Español, P. Warren, Statistical mechanics of dissipative particle dynamics, Europhys. Lett. 30 (1995) 191–196.
[13] P. Hoogerbrugge, J. Koelman, Simulating microscopic hydrodynamic phenomena with dissipative particle dynamics, Europhys. Lett 19 (1992) 155–160.
[14] B. Oksendal, Stochastic Differential Equations, 5th Edition, Springer-Verlag, Berlin-Heidelberg, 2000.
[15] C. Cotter, S. Reich, An extended dissipative particle dynamics model, Europhys. Lett. 64 (2003) 723–729.
[16] P. Español, Dissipative Particle Dynamics, in: V. Harik, M. Salas (Eds.), Trends in nanoscale mechanics: Analysis of nanostructure materials and multi-scale modeling, Kluwer, 2003, pp. 1–23.
[17] E. Koopman, C. Lowe, Advantages of a Lowe-Andersen thermostat in molecular dynamics simulations, J. Chem. Phys. 124 (2006) 204103.
[18] L. Verlet, Computer experiments on classical fluids. I. Thermodynamical properties of Lennard-Jones molecules, Phys. Lett. 159 (1967) 98–103.
[19] R. Skeel, D. Hardy, Practical construction of modified Hamiltonians, SIAM J. Sci. Comput. 23 (2001) 1172–1188.
[20] R. Engle, R. Skeel, M. Drees, Monitoring energy drift with shadow hamiltonians, J. Comput. Phys. 206 (2005) 432–452.
[21] J. Izaguirre, S. Hampton, Shadow Hybrid Monte Carlo: An efficient propagator in phase space of macromolecules, J. Comput. Phys. 200 (2004) 581–604.
[22] I. Pagonabarraga, M. Hagen, D. Frenkel, Self-consistent dissipative particle dynamics, Europhys. Lett. 42 (1998) 377–382.
[23] C. Lowe, An alternative approach to dissipative particle dynamics, Europhys. Lett. 47 (1999) 145–151.
[24] G. Besold, I. Vattulainen, M. Karttunen, J. Polson, Towards better integrators for dissipative particle dynamics, Phys. Rev. E 62 (2000) R7611–R7614.
[25] T. Shardlow, Splitting for dissipative particle dynamics, SIAM J. Sci. Comput. 24 (2003) 1267–1282.
[26] I. Vattulainen, M. Karttunen, B. Besold, J. Polson, Integration schemes for dissipative particle dynamics simulations: From softly interacting systems towards hybrid models, J. Chem. Phys. 116 (2002) 3967–3979.
[27] P. Nikunen, M. Karttunen, I. Vattulainen, How would you integrate the equations of motion in dissipative particle dynamics, Computer Physics Communications 153 (2003) 407–423.
[28] E. Peters, Elimination of time step effects in DPD, Europhys. Lett. 66 (2004) 311–317.
[29] B. Hafskjold, C. Liew, W. Shinoda, Can such long time steps really be used in Dissipative Particle Dynamics simulations, Mol. Sim. 30 (2004) 879–885.
[30] M. Serrano, G. D. Fabritiis, P. Español, P. Coveney, A stochastic Trotter integration scheme for dissipative particle dynamics, Mathematics and Computers in Simulation 72 (2006) 190–194.
[31] R. Skeel, Integration schemes for molecular dynamics and related applications, in: M. Ainsworth, J. Levesley, M. Marletta (Eds.), The Graduate Student's Guide to Numerical Analysis, Vol. 4 of SSCM, Springer-Verlag, Berlin, 1999, pp. 119–176.
[32] J. Izaguirre, D. Catarello, J. Wozniak, R. Skeel, Langevin stabilization of molecular dynamics, J. Chem. Phys. 114 (2001) 2090–2098.
[33] R. Skeel, J. Izaguirre, An impulse integrator for Langevin dynamics, Mol. Phys. 100 (2002) 3885–3891.
[34] G. D. Fabritis, M. Serrano, P. Español, P. Coveney, Efficient numerical integrators for stochastic models, Physica A 361 (2006) 429–440.
[35] G. Bussi, M. Parrinello, Accurate sampling using Langevin dynamics, Physical Review E 75 (2007) 056707.
[36] S. Duane, A. Kennedy, B. Pendleton, D. Roweth, Hybrid Monte-Carlo, Phys. Lett. B 195 (1987) 216–222.
[37] B. Mehlig, D. Heermann, B. Forrest, Hybrid Monte Carlo method for condensed-matter systems, Phys. Rev. B 45 (1992) 679–685.
[38] E. Akhmatskaya, N. Bou-Rabee, S. Reich, Generalized hybrid Monte Carlo methods without momentum flip, J. Comput. Phys. 228 (2009) 2256–2265.
[39] E. Akhmatskaya, S. Reich, Erratum for "generalized hybrid Monte Carlo methods without momentum flip", J. Comput. Phys. 228 (2009) 7492–7496.
[40] B. Leimkuhler, S. Reich, A Metropolis adjusted Nosé-Hoover thermostat, M2AN 43 (2009) 743–755.
[41] B. Leimkuhler, E. Noorizadeh, F. Theil, A gentle ergodic thermostat for molecular dynamics, J. Stat. Phys. 135 (2009) 261–277.
[42] P. Bond, M. Sansom, Insertion and assembly of membrane proteins via simulation, J. Amer. Chem. Soc. 128 (2006) 2697–2704.
[43] P. Bond, J. Holyoake, A. Ivetac, S. Khalid, M. Sansom, Coarse-grained molecular dynamics simulations of membrane proteins and peptides, J. Struct. Biol. 157 (2007) 593–605.
[44] A. Shih, A. Arkhipov, P. Freddolino, K. Schulten, Coarse grained protein-lipid model with application to lipoprotein particles, J. Phys. Chem. B 110 (8) (2006) 3674–3684.
[45] C. Wee, M. Sansom, S. Reich, E. Akhmatskaya, Improved sampling for simulations of interfacial membrane proteins: Application of GSHMC to a peptide toxin/bilayer system, J. Phys. Chem. B 112 (2008) 5710–5717.